

Occupation deficiency in layered structures of UNi_xSb_2 ($0 \leq x \leq 1$) studied by density functional theory supercell calculations

M. Werwiński*, A. Szajek

*Institute of Molecular Physics, Polish Academy of Sciences,
ul. M. Smoluchowskiego 17, 60-179 Poznań, Poland*

Abstract

The five crystal structures of selected UNi_xSb_2 compositions are investigated by density functional theory supercell calculations. The considered phases are USb_2 , $\text{UNi}_{0.33}\text{Sb}_2$, $\text{UNi}_{0.5}\text{Sb}_2$, $\text{UNi}_{0.66}\text{Sb}_2$, and UNiSb_2 ($x = 0, 1/3, 1/2, 2/3, 1$). The occupation deficiency of Ni is modeled by removing the Ni layers from constructed supercells followed by relaxation of the structures. A linear dependence of the lattice parameter c versus Ni concentration x is observed, same fulfilling the empirical Vegard's law. The agreement between results of our calculations with the empirical data from literature confirms the validity of our approach of supercells with empty Ni layers at least in predicting of lattice parameters. The calculated with orbital polarization magnetic moments on uranium atoms decrease from $1.70 \mu_B$ to $1.61 \mu_B$ with increasing Ni concentration x . In comparison to available empirical data of USb_2 and $\text{UNi}_{0.5}\text{Sb}_2$, the magnetic moments calculated with orbital polarization are less than 10% smaller.

Keywords: Layered structures, Uranium compounds, *Ab initio* calculations, DFT, Geometry optimization, Supercells

1. Introduction

Since the discovery of graphene in 2004 the two-dimensional systems of its analogs have been intensively studied. Parallel to these efforts also the bulk layered materials have attracted the great attention. Some of the recent studies focus on the new layered superconductors like BiS_2 [1], LaXPO ($X = \text{Mn, Fe, Ni}$) [2], and $(\text{Ca,Pr})\text{FeAs}_2$ [3] or the cathode materials for advanced rechargeable Na-ion batteries Na_xMO_2 [4, 5]. The Na_xMO_2 is also an example of a system with occupation deficiency in a layered structure. Some other samples of layered materials with occupation deficiency are uranium ternaries like $\text{UFe}_{0.6}\text{Sb}_2$ [6] (UFeSb_2 [7]) and $\text{UCu}_{0.83}\text{Sb}_2$ [8]. But it is the $\text{UNi}_{0.5}\text{Sb}_2$ phase which physical properties are studied particularly intensively. [9, 10, 11, 12, 13, 14, 15] Some of our previous studies on uranium ternaries addressed similar phases i.e. UCuSb_2 [16], UCu_2Si_2 [17], or URu_2Si_2 [18]. In this work we investigate the crystal structures of selected UNi_xSb_2 compositions ($x = 0, 1/3, 1/2, 2/3, 1$) by density functional theory supercell calculations. The occupation deficiency of Ni is modeled by a removal of whole Ni layers from constructed supercells which is followed by a relaxation of the structures. In this paper we will present the calculated crystal structures and compare their parameters to the empirical data from literature. We will also show the results of

the magnetic moments calculations for antiferromagnetic UNi_xSb_2 structures. Our method of preparation of the supercells can serve to other experimental and theoretical groups which are dealing with layered materials with occupation deficiency.

2. Details of calculations

For *ab initio* calculations we used the full potential linearized augmented plane wave FP-LAPW method as implemented in the WIEN2k code [19] with the exchange-correlation potential in the Perdew–Burke–Ernzerhof (PBE) form. [20] The spin-orbit coupling does not play an important role in the optimization of the crystal structure, so we included only scalar relativistic effects for the optimization. In order to get a sufficient accuracy we set the parameters of computations relatively high: the total energy convergence criterion was 10^{-7} Ry, the plane wave cut-off parameter was $RK_{max} = 8$, the numbers of \mathbf{k} -points in the irreducible wedges of the Brillouin zones were: 256 ($16 \times 16 \times 7$) for UNiSb_2 , 110 ($20 \times 20 \times 4$) for $\text{UNi}_{0.5}\text{Sb}_2$, 43 ($13 \times 13 \times 2$) for $\text{UNi}_{0.33}\text{Sb}_2$ and $\text{UNi}_{0.66}\text{Sb}_2$, and 171 ($20 \times 20 \times 9$) for USb_2 , the muffin-tin radii were $r_U = 2.5$, $r_{Ni} = 2.33$, and $r_{Sb} = 2.33 a_0$, and the force convergence criterion was 10^{-3} Ry/ a_0 . To calculate the magnetic moments we included the spin-orbit coupling term for all orbitals and the orbital polarization corrections [21, 22] for U $5f$ and Ni $3d$ orbitals. The crystal structures were visualized with VESTA. [23]

*Corresponding author

Email address: werwinski@ifmpan.poznan.pl (M. Werwiński)

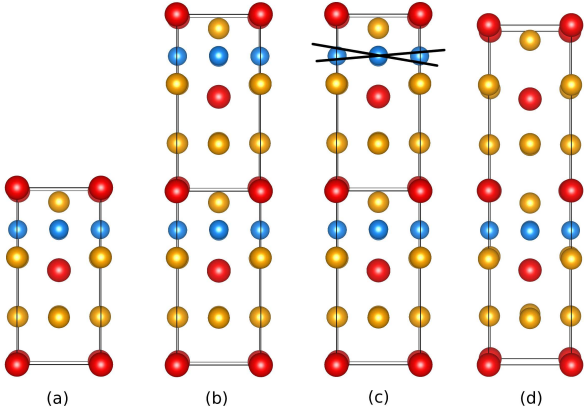


Figure 1: The four steps of preparation of the supercell model with the occupation deficiency, based on the structure of the $\text{UNi}_{0.5}\text{Sb}_2$ as an example. a) Starting with a fully occupied single unit cell; b) multiplication of the fully occupied unit cell along the z direction; c) removal of the atomic layers in order to reproduce the target concentration; d) structure optimization by *ab initio* calculations. The red color is used for U, blue for Ni, and orange for Sb.

Table 1: Experimental crystal data for USb_2 [26] and UNiSb_2 . [24] Experimental Wyckoff positions z_U and z_{As} for UNiAs_2 isostructural to UNiSb_2 are $z_U = 0.2456(4)$ and $z_{Sb} = 0.6531(4)$. [25]

phase	USb_2	UNiSb_2
sg.	$P4/nmm$	$P4/nmm$
a (Å)	4.272	4.322(1)
c (Å)	8.741	9.081(1)
U (2c)	1/4 1/4 0.280	1/4 1/4 z_U
Sb (2a)	1/4 3/4 0	3/4 1/4 0
Sb (2c)	3/4 3/4 0.365	1/4 1/4 z_{Sb}
Ni (2b)		3/4 1/4 1/2

The preparation of all considered UNi_xSb_2 crystallographic models starts from the experimental crystallographic data for a fully occupied unit cell of UNiSb_2 [24, 25], see Tab. 1 and Fig. 2 d). In Tab. 1 we present also the experimental crystal data for USb_2 [26].

The important problem which we had to address is how to model the occupation deficiency in considered UNi_xSb_2 compositions. One way would be to use the coherent potential approximation CPA [27] by alloying Ni with empty spheres. The other way would be to treat the deficiencies as point defects and prepare the supercells [28] with vacancies, as it has been done for an isostructural $\text{UCu}_{0.75}\text{Sb}_2$ phase. [8] However taking into account a linear behavior of $c(x)$ observed for UCu_xSb_2 [29], we decided to use the supercell approach treating the Ni deficiencies as planar defects. Our method can be summarized in four steps: a) start with a fully occupied single unit cell (in our case UNiSb_2); b) multiply the fully occupied unit cell along the z direction; c) remove the atomic layers in order to reproduce the target concentration; d) use the *ab initio* calculations to optimize the structures. A sketch of our

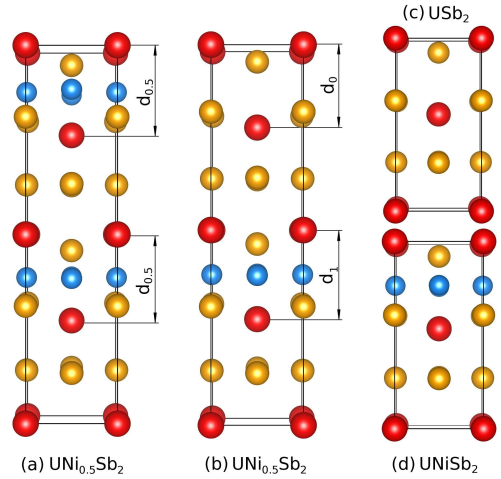


Figure 2: The (a) experimentally [14] and (b) theoretically predicted crystal structures of $\text{UNi}_{0.5}\text{Sb}_2$. (c) USb_2 and (d) UNiSb_2 crystal structures. The red spheres represent U atoms, the blue Ni, and the orange Sb. In the experimental structure of $\text{UNi}_{0.5}\text{Sb}_2$ (a) every Ni layer is half-occupied. In the proposed model (b) of $\text{UNi}_{0.5}\text{Sb}_2$ one of two Ni layers is removed and the other is fully occupied. The theoretical model (b) of $\text{UNi}_{0.5}\text{Sb}_2$ can be considered as a combination of the USb_2 (c) and UNiSb_2 (d) crystal structures.

method is also presented in Fig. 1.

3. Results and discussion

We noticed that the lattice parameter c versus Cu concentration x for the UCu_xSb_2 system is linear obeying the Vegard's law [29] when the lattice parameter a versus x remains more or less the same, see Fig. 3. It led us to the assumption that the Ni deficiency in layered UNi_xSb_2 system takes the form of vacating full Ni layers perpendicular to a tetragonal axis. We then proposed the simplified model of $\text{UNi}_{0.5}\text{Sb}_2$ which consists of two combined unit cells, one with a full Ni layer and the other with an empty one, which looks like a combination of UNiSb_2 and USb_2 unit cells, see Fig. 1 c). A further support for our reasoning comes from the experimental data, where the sum of USb_2 and UNiSb_2 lattice parameters c $8.741 + 9.081 = 17.822$ (Å) [26, 24] is very close to the value of $c = 17.868$ Å for $\text{UNi}_{0.5}\text{Sb}_2$. [14] Based on the above arguments we decided to model the UNi_xSb_2 layered compounds with occupation deficiency as composed of unit cells with completely full or empty Ni layers in right proportion to Ni concentration. The main result of this work are five crystal structures predicted for USb_2 , $\text{UNi}_{0.33}\text{Sb}_2$, $\text{UNi}_{0.5}\text{Sb}_2$, $\text{UNi}_{0.66}\text{Sb}_2$, and UNiSb_2 . The structures data are collected in Tab. 2.

We start the calculations from relaxation of the experimental unit cell of UNiSb_2 [24, 25], see Tab. 1 and Fig. 2 d). The UNiSb_2 unit cell contains a single Ni layer perpendicular to the c axis. The fact that the UNiSb_2 is an antiferromagnet (AFM) [30] has to be taken into account in order to get an accurate result of the relaxation. We do this by lowering the symmetry of the unit cell of UNiSb_2 and con-

Table 2: The crystallographic data of theoretically predicted crystal structures for USb_2 , $\text{UNi}_{0.33}\text{Sb}_2$, $\text{UNi}_{0.5}\text{Sb}_2$, $\text{UNi}_{0.66}\text{Sb}_2$, and UNiSb_2 compounds.

phase	$\text{UNi}_{0.33}\text{Sb}_2$	phase	$\text{UNi}_{0.5}\text{Sb}_2$	phase	$\text{UNi}_{0.66}\text{Sb}_2$	phase	UNiSb_2
sg.	P4mm	sg.	P4mm	sg.	P4mm	sg.	P4/nmm
a (Å)	4.32	a (Å)	4.33	a (Å)	4.32	a (Å)	4.32
c (Å)	26.60	c (Å)	17.84	c (Å)	26.95	c (Å)	9.11
U1	0.75 0.75 0.235	U1	0.0 0.0 0.000	U1	0.75 0.75 0.248	U(2c)	0.25 0.25 0.267
U2	0.75 0.75 0.582	U2	0.5 0.5 0.275	U2	0.75 0.75 0.571	Ni(2b)	0.75 0.25 0.500
U3	0.75 0.75 0.908	U3	0.0 0.0 0.513	U3	0.75 0.75 0.909	Sb1(2a)	0.75 0.25 0.000
U4	0.25 0.25 0.092	U4	0.5 0.5 0.788	U4	0.25 0.25 0.091	Sb2(2c)	0.25 0.25 0.660
U5	0.25 0.25 0.419	Sb1	0.0 0.5 0.137	U5	0.25 0.25 0.429	phase	USb_2
U6	0.25 0.25 0.766	Sb2	0.0 0.0 0.312	U6	0.25 0.25 0.752	sg.	P4/nmm
Sb1	0.25 0.25 0.210	Sb3	0.5 0.5 0.476	Sb1	0.25 0.25 0.224	a (Å)	4.326
Sb2	0.75 0.75 0.117	Sb4	0.5 0.0 0.651	Sb2	0.75 0.75 0.114	c (Å)	8.707
Sb3	0.25 0.25 0.556	Sb5	0.0 0.0 0.824	Sb3	0.25 0.25 0.546	U1(2c)	0.25 0.25 0.281
Sb4	0.75 0.75 0.445	Sb6	0.5 0.5 0.964	Sb4	0.75 0.75 0.454	Sb1(2a)	0.25 0.75 0.000
Sb5	0.25 0.25 0.884	Ni1	0.5 0.0 0.394	Sb5	0.25 0.25 0.886	Sb2(2c)	0.75 0.75 0.358
Sb6	0.75 0.75 0.791			Sb6	0.75 0.75 0.776		
Sb7	0.25 0.75 0.000			Sb7	0.25 0.75 0.000		
Sb8	0.25 0.75 0.327			Sb8	0.25 0.75 0.339		
Sb9	0.25 0.75 0.674			Sb9	0.25 0.75 0.661		
Ni1	0.25 0.75 0.500			Ni1	0.25 0.75 0.168		
				Ni2	0.25 0.75 0.832		

sidering two inequivalent U sites as carrying the opposite magnetic moments. The lattice parameter $c = 9.110$ Å calculated from AFM UNiSb_2 structure agrees much better with the experimental value $c = 9.081$ Å [24] than the theoretical non-magnetic result $c = 8.991$ Å. We conclude that for the UNi_xSb_2 phases the relaxation should be conducted in AFM spin-polarized mode.

The first structure calculated by us based on the supercell method is the USb_2 structure, see Fig. 2 c) and Tab. 2. USb_2 can be considered as an extreme member of the UNi_xSb_2 family with the Ni occupation equal to zero. To model it we have removed the only Ni layer from UNiSb_2 single unit cell and optimized the structure. After the AFM relaxation performed with no symmetry we determined for USb_2 the P4/nmm space group, consistent with the experiment. The fact that the calculated space group, lattice parameters, and Wyckoff positions z_U and z_{Sb} are all in excellent agreement with measured values (see Tables 2 and 1) confirms the validity of the introduced supercell method.

The second layered structure with occupation deficiency calculated with our method is the structure of the $\text{UNi}_{0.5}\text{Sb}_2$, see Tab. 2. The $\text{UNi}_{0.5}\text{Sb}_2$ is an antiferromagnet with the Néel temperature $T_N = 161$ K, its magnetic moments are localized on uranium atoms and oriented along the c axis [31] with ordering sequence $+ - + -$. [14] The $\text{UNi}_{0.5}\text{Sb}_2$ structure was described in literature twice, the first approach [31] is based on a single UNiSb_2 -type unit cell and describes the Ni occupation as close to 0.5. The second approach by Torikachvili et al. [14] is based

on a doubled UNiSb_2 -type unit cell containing two half-filled Ni layers, see Fig. 2 a). In this picture the space group is $P4_2/nmc$ and the lattice parameters following $a = 4.333(6)$ Å and $c = 17.868(4)$ Å and the interlayer U-U distance $d_{0.5} = 4.15$ Å. The crystal structure of $\text{UNi}_{0.5}\text{Sb}_2$ generated with our supercell method has a space group P4mm and lattice parameters $a = 4.336$ Å and $c = 17.837$ Å, see Fig. 2 b). Although we observe a very good consistency between lattice parameters from the experimental and theoretical pictures, the corresponding two sets of atomic positions significantly differ. In our picture the top Ni layer is emptied and the bottom one is full, see Fig. 2 b). The calculated interlayer U-U distances $d_0 = 3.79$ Å and $d_1 = 4.25$ Å, for empty and full Ni layers, correspond well to the U-U distances for USb_2 and UNiSb_2 ($d_{\text{USb}_2} = 3.82$ Å and $d_{\text{UNiSb}_2} = 4.24$ Å). It shows how close our picture of $\text{UNi}_{0.5}\text{Sb}_2$ is to the one combined of USb_2 and UNiSb_2 .

As we can see in Fig. 3, the calculated linear behavior of $c(x)$ for UNi_xSb_2 phase diagram is in excellent agreement with experimental data from literature. Linear regression analysis leads to the formula $c = 8.71 + 0.40x$ (Å) for $c(x)$ calculations for UNi_xSb_2 and $c = 8.75 + 0.33x$ (Å) for corresponding experimental data. For isostructural UCu_xSb_2 also the linear behavior is observed following a formula $c = 8.77 + 0.88x$ (Å). The above result can be also compared with a relation found experimentally for a martensite with a tetragonal distortion $c_{FeC} = 2.87 + 0.116x_C$ (Å), where the lattice parameter c is proportional to the amount of carbon x_C in the alloy (for small C concen-

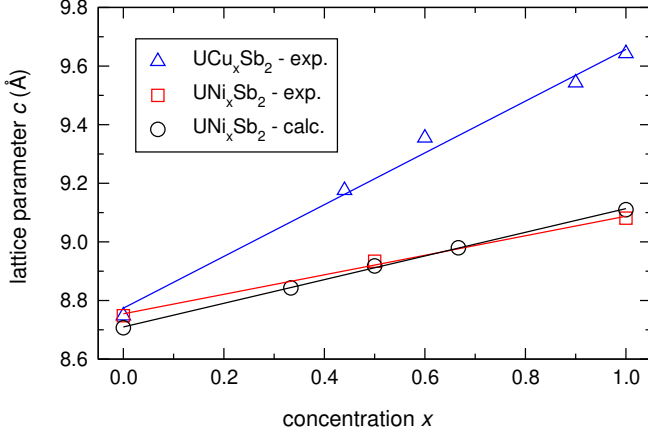


Figure 3: The calculated dependence of lattice parameter c versus Ni concentration x for UNi_xSb_2 system. For comparison the corresponding experimental results for UNi_xSb_2 [26, 14, 24] and for UCu_xSb_2 [26, 32, 29, 11, 24] systems. The experimental results for UCu_xSb_2 have been for the first time collected by Ringe and Ibers. [29] Symbols are for data points and straight lines for linear regression.

trations). [33, 34] The calculated linear behavior of $c(x)$ for UNi_xSb_2 is a strong evidence that our approach is a suitable method of modeling the layered structures with occupation deficiency. It can be used both to improve structure determination with XRD and as an independent theoretical tool.

The presented approach of structure modeling is supported by the results of calculated magnetic moments. For the proposed supercell model of $\text{UNi}_{0.5}\text{Sb}_2$ we consider three uniaxial antiferromagnetic configurations: $+ - + -$, $++ - -$, and $+ - - +$, see Fig. 4. The calculations with PBE approximation and spin-orbit coupling lead to the lowest total energy for $+ - + -$ antiferromagnetic structure and the $++ - -$ and $+ - - +$ configurations are 49 and 27 meV per unit cell higher in total energy, respectively. For the unfavorable $++ - -$ configuration the two layers of U atoms adjacent to the layer of Ni are oriented ferromagnetically, thus induce a small magnetic moment of $0.08 \mu_B$ on Ni atoms.

We calculate also the magnetic moments for the antiferromagnetic structures of all considered UNi_xSb_2 structures ($x = 0, 1/3, 1/2, 2/3, 1$). The calculated spin (m_s), orbital (m_l), and total (m_j) magnetic moments on uranium atoms are presented in Tab. 3. One set of results (PBE) is based on the simple PBE approximation, another set (PBE+OP) is obtained with the additional potential called orbital polarization (OP) in the form introduced by Brooks, Johansson, and Eriksson [21, 22] and with OP parameters calculated *ab initio*. For the both sets the spin-orbit coupling is included. As some of the considered structures have more than one pair of antiferromagnetically coupled U atoms, we evaluate also the average values of the magnetic moments on U atoms. The total magnetic moments on U atom $|\tilde{m}_j(\text{U})|$ for basic composition USb_2 is equal $1.03 \mu_B$ in the PBE approach and it comprises

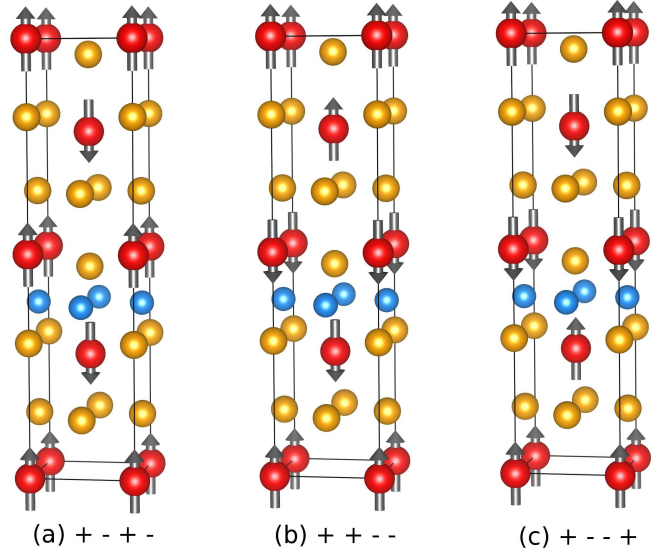


Figure 4: Three antiferromagnetic structures of $\text{UNi}_{0.5}\text{Sb}_2$ based on the proposed supercell model with occupation deficiency. The considered uniaxial antiferromagnetic configurations are (a) $+ - + -$, (b) $++ - -$, and (c) $+ - - +$.

Table 3: The calculated spin (m_s), orbital (m_l), and total (m_j) magnetic moments on uranium atoms ($\text{U}_1, \text{U}_2, \text{U}_3$) for $\text{USb}_2, \text{UNi}_{0.33}\text{Sb}_2, \text{UNi}_{0.5}\text{Sb}_2, \text{UNi}_{0.66}\text{Sb}_2,$ and UNiSb_2 compounds. The corresponding magnetic moments averaged over the contributing uranium atoms are also presented. Two presented sets of results are obtained with the Perdew–Burke–Ernzerhof (PBE) exchange–correlation potential. For the second set we included an additional orbital polarization (OP) for U $5f$ and Ni $3d$ orbitals.

		x	0	0.33	0.5	0.66	1	
PBE	U_1	m_s	1.56	1.67	1.68	1.63	1.63	
		m_l	-2.59	-2.68	-2.68	-2.20	-2.19	
		m_j	-1.03	-1.00	-1.00	-0.57	-0.56	
	U_2	m_s		1.63	1.63	1.66		
		m_l		-2.24	-2.22	-2.66		
		m_j		-0.61	-0.59	-1.00		
	U_3	m_s		1.65		1.63		
		m_l		-2.67		-2.21		
		m_j		-1.02		-0.58		
			\tilde{m}_s	1.56	1.65	1.65	1.64	1.63
			\tilde{m}_l	-2.59	-2.53	-2.45	-2.36	-2.19
			$ \tilde{m}_j $	1.03	0.88	0.79	0.72	0.56
PBE+OP	U_1	m_s	1.79	1.88	1.89	1.88	1.85	
		m_l	-3.49	-3.59	-3.59	-3.53	-3.46	
		m_j	-1.70	-1.72	-1.70	-1.65	-1.61	
	U_2	m_s		1.88	1.87	1.86		
		m_l		-3.53	-3.53	-3.56		
		m_j		-1.65	-1.66	-1.70		
	U_3	m_s		1.87		1.86		
		m_l		-3.59		-3.48		
		m_j		-1.72		-1.62		
			\tilde{m}_s	1.79	1.87	1.88	1.86	1.85
			\tilde{m}_l	-3.49	-3.57	-3.56	-3.52	-3.46
			$ \tilde{m}_j $	1.70	1.69	1.68	1.66	1.61

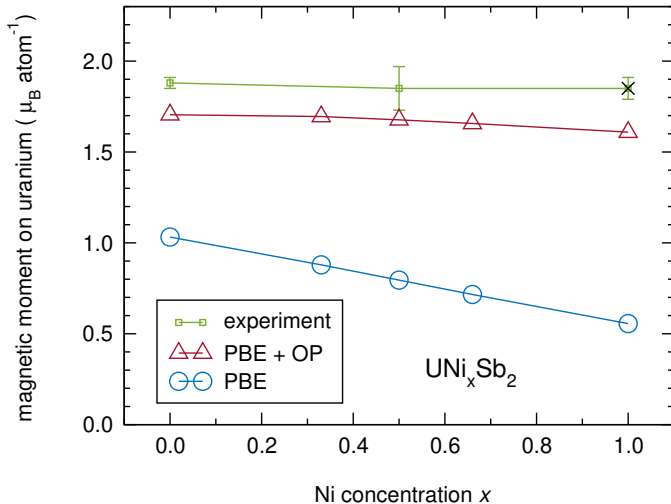


Figure 5: The calculated dependence of average total magnetic moment on uranium atom *versus* Ni concentration x for UNi_xSb_2 system. The corresponding experimental results for USb_2 [35], $\text{UNi}_{0.5}\text{Sb}_2$ [14], and an isostructural (marked with cross) UNiAs_2 [25] are presented for comparison. Two sets of results are obtained with the Perdew–Burke–Ernzerhof (PBE) exchange-correlation potential, for one of them we additionally included the orbital polarization (OP).

of spin $\tilde{m}_s(\text{U}) = 1.56 \mu_B$ and orbital $\tilde{m}_l(\text{U}) = -2.59 \mu_B$ magnetic moments. The corresponding values obtained in the PBE+OP approach are 1.70, 1.79, and $-3.49 \mu_B$, respectively. In comparison to the simple PBE, the orbital polarization increases significantly the orbital contribution, simultaneously increasing the total magnetic moment. Similar results for other compositions are collected in Tab. 3. Figure 5 presents the calculated dependencies of $|\tilde{m}_j(\text{U})|$ *versus* Ni concentration x . For the PBE and PBE+OP approaches we observe a decrease of the magnetic moment with x . Although, for the PBE+OP the drop is much lower and the values of magnetic moment on U better correspond to the experimental results for USb_2 ($1.88 \pm 0.03 \mu_B$) [35], $\text{UNi}_{0.5}\text{Sb}_2$ ($1.85 \pm 0.12 \mu_B$) [14], and an isostructural UNiAs_2 ($1.85 \pm 0.06 \mu_B$) [25]. For the $\text{UNi}_{0.5}\text{Sb}_2$ the magnetic moment on U calculated with PBE+OP ($1.68 \mu_B$) is smaller than the experimental one ($1.85 \pm 0.12 \mu_B$). [14]

4. Summary and conclusions

The problem of modeling of the layered structures with occupation deficiency was addressed with the method based on the supercells. It can be summarized in four steps: a) start with a fully occupied single unit cell; b) multiply it along the z direction; c) remove the proper atomic layers; d) optimize the structures. We proved the utility of the supercell method by predicting the five crystal structures of the UNi_xSb_2 phase diagram ($x = 0, 1/3, 1/2, 2/3, 1$). The credibility of the method was confirmed by comparison of the evaluated $c(x)$ plot with the corresponding experimental results from literature. Based on

the obtained supercells of UNi_xSb_2 and including the orbital polarization corrections we also calculated the magnetic moments on uranium atoms. The presented method of modeling can be applied to support the XRD analysis where the calculated model can be used as an initial structure to an experimental fit. The calculated structures of the UNi_xSb_2 phase diagram can be used for further electronic structure calculations or as the basis models for the isostructural phases.

5. Acknowledgements

The authors would like to thank professor Peter Oppeneer for helpful discussion and comments. MW acknowledges the financial support from the Foundation of Polish Science grant HOMING. The HOMING programme is co-financed by the European Union under the European Regional Development Fund.

6. Bibliography

References

- [1] Y. Mizuguchi, *Journal of Physics and Chemistry of Solids Focus issue on the Study of matter at extreme conditions and related phenomena*, **84**, 34 (2015).
- [2] H. A. Rahnamaye Aliabad, H. Akbari, and M. A. Saeed, *Computational Materials Science* **106**, 5 (2015).
- [3] H. Yakita, H. Ogino, T. Okada, A. Yamamoto, K. Kishio, T. Tohei, Y. Ikuhara, Y. Gotoh, H. Fujihisa, K. Kataoka, H. Eisaki, and J.-i. Shimoyama, *Journal of the American Chemical Society* **136**, 846 (2014).
- [4] J. Su, Y. Pei, Z. Yang, and X. Wang, *Computational Materials Science* **98**, 304 (2015).
- [5] G. Li, X. Yue, G. Luo, and J. Zhao, *Computational Materials Science* **106**, 15 (2015).
- [6] D. Xie, W. Zhang, Q. Liu, Y. Liu, S. Tan, W. Feng, Y. Zhang, Y. Zhang, X. Zhu, Q. Chen, L. Luo, B. Yuan, B. Wang, and X. Lai, *Journal of Alloys and Compounds* **663**, 672 (2016).
- [7] A. P. Gonçalves, M. S. Henriques, J. C. Waerenborgh, I. Curlik, S. Il'kovič, and M. Reiffers, *Journal of Alloys and Compounds* **616**, 601 (2014).
- [8] M. Samsel-Czekala, E. Talik, M. J. Winiarski, and R. Troć, *Journal of Alloys and Compounds* **638**, 313 (2015).
- [9] T. Plackowski, D. Kaczorowski, and Z. Bukowski, *Physical Review B* **72**, 184418 (2005).
- [10] Z. Bukowski, K. Gofryk, T. Plackowski, and D. Kaczorowski, *Journal of Alloys and Compounds* **400**, 33 (2005).
- [11] Z. Bukowski, R. Troć, J. Stępień-Damm, C. Sułkowski, and V. H. Tran, *Journal of Alloys and Compounds* **403**, 65 (2005).
- [12] J. Mucha, H. Misiorek, R. Troć, and Z. Bukowski, *Journal of Physics: Condensed Matter* **18**, 3097 (2006).
- [13] B. K. Davis, M. S. Torikachvili, E. D. Mun, J. C. Frederick, G. J. Miller, S. Thimmaiah, S. L. Bud'ko, and P. C. Canfield, *Journal of Applied Physics* **103**, 07B704 (2008).
- [14] M. S. Torikachvili, B. K. Davis, K. Kothapalli, H. Nakotte, A. J. Schultz, E. D. Mun, and S. L. Bud'ko, *Physical Review B* **84**, 205114 (2011).
- [15] R. Troć and R. Wawryk, *Intermetallics* **60**, 72 (2015).
- [16] M. Werwiński, A. Szajek, and J. A. Morkowski, *Computational Materials Science* **81**, 402 (2014).
- [17] J. A. Morkowski, G. Chełkowska, M. Werwiński, A. Szajek, R. Troć, and C. Neise, *Journal of Alloys and Compounds* **509**, 6994 (2011).
- [18] M. Werwiński, J. Rusz, J. A. Mydosh, and P. M. Oppeneer, *Physical Review B* **90**, 064430 (2014).

- [19] Peter Blaha, Karlheinz Schwarz, Georg Madsen, Dieter Kvasnicka, and Joachim Luitz, “WIEN2k An Augmented Plane Wave Plus Local Orbitals Program for Calculating Crystal Properties,” (2014).
- [20] J. P. Perdew, K. Burke, and M. Ernzerhof, *Physical review letters* **77**, 3865 (1996).
- [21] M. S. S. Brooks, *Physica B+C* **130**, 6 (1985).
- [22] O. Eriksson, M. S. S. Brooks, and B. Johansson, *Physical Review B* **41**, 7311 (1990).
- [23] K. Momma and F. Izumi, *Journal of Applied Crystallography* **41**, 653 (2008).
- [24] D. Kaczorowski, R. Kruk, J. P. Sanchez, B. Malaman, and F. Wastin, *Physical Review B* **58**, 9227 (1998).
- [25] P. Fischer, A. Murasik, D. Kaczorowski, and R. Troć, *Physica B: Condensed Matter* **156**, 829 (1989).
- [26] J. Leciejewicz, R. Troć, A. Murasik, and A. Zygmunt, *physica status solidi (b)* **22**, 517 (1967).
- [27] A. Edström, M. Werwiński, D. Iuşan, J. Ruzs, O. Eriksson, K. P. Skokov, I. A. Radulov, S. Ener, M. D. Kuz'min, J. Hong, M. Fries, D. Y. Karpenkov, O. Gutfleisch, P. Toson, and J. Fidler, *Physical Review B* **92**, 174413 (2015).
- [28] L. Reichel, L. Schultz, D. Pohl, S. Oswald, S. Fähler, M. Werwiński, A. Edström, E. K. Delczeg-Czirjak, and J. Ruzs, *Journal of Physics: Condensed Matter* **27**, 476002 (2015).
- [29] E. Ringe and J. A. Ibers, *Acta Crystallographica Section C Crystal Structure Communications* **64**, i76 (2008).
- [30] D. Kaczorowski, *Journal of Alloys and Compounds* **186**, 333 (1992).
- [31] Z. Bukowski, D. Kaczorowski, J. Stepień-Damm, D. Badurski, and R. Troć, *Intermetallics* **12**, 1381 (2004).
- [32] S. Bobev, D. J. Mixson, E. D. Bauer, and J. L. Sarrao, *Acta Crystallographica Section E Structure Reports Online* **62**, i66 (2006).
- [33] G. V. Kurdjumov and A. G. Khachaturyan, *Acta Metallurgica* **23**, 1077 (1975).
- [34] E. K. Delczeg-Czirjak, A. Edström, M. Werwiński, J. Ruzs, N. V. Skorodumova, L. Vitos, and O. Eriksson, *Physical Review B* **89**, 144403 (2014).
- [35] S. Tsutsui, M. Nakada, S. Nasu, Y. Haga, D. Aoki, P. Wiśniewski, and Y. Ōnuki, *Physical Review B* **69** (2004), 10.1103/PhysRevB.69.054404.